J. Am. Soc. Mass Spectrom. (2017) 28:2352–2360
DOI: 10.1007/s13361-017-1765-1

RESEARCH ARTICLE

TOF MS Investigation of Nickel Oxide CVD

Anastasia S. Kondrateva, Maxim V. Mishin, Sergey E. Alexandrov

Department of Physical Chemistry and Microsystem Technology, Peter the Great Saint Petersburg State Polytechnic University, Polytechnicheskaya str. 29, St. Petersburg, 195251, Russian Federation

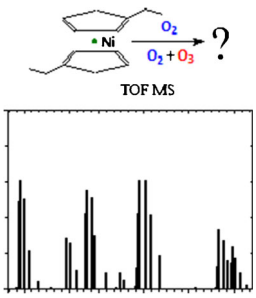

Abstract. NiO layers were deposited by metal-organic chemical vapor deposition using bis-(ethylcyclopentadienyl) nickel $(EtCp)_2Ni$ and oxygen or ozone. As a continuation of kinetic study of NiO MOCVD the gas-phase, transformations of $(EtCp)_2Ni$ were studied in the temperature range of 380–830 K. Time of reactions corresponding to the residence time of the gas stream in hot zone of the reactor was about 0.1 s under conditions studied. The interaction of $(EtCp)_2Ni$ with oxygen started at 450 K and its conversion rate reached the maximum at 700 K. The interaction of $(EtCp)_2Ni$ with ozone started at 400 K and its conversion rate reached the maximum at 600 K. Transformations of the gas phase with the temperature in the reaction zone were studied, the model reaction schemes illustrating $(EtCp)_2Ni$ transformations in the reaction systems containing oxygen and ozone have developed. In the reaction system $(EtCp)_2Ni–O_2–Ar$ the main gas-phase products at 380–500 K were CO, CO_2, HCO, C_2H_5OH, CpCOOH, and CpO. Formation of the C_2H_2O, C_3H_4O, and C_5H_8O was found at 630–830 K. The same gas-phase species, $(C_4H_3O)_2Ni$ and dialdehydes was formed in the reaction system $(EtCp)_2Ni–O_3–O_2–Ar$.

Keywords: Gas-phase, bis-(ethylcyclopentadienyl) nickel, MOCVD, NiO, Reaction scheme

Received: 11 May 2017/Revised: 18 July 2017/Accepted: 18 July 2017/Published Online: 11 August 2017

Introduction

NiO layers have attracted considerable interest of scientists because of the wide range of their potential applications, such as sensing layers in semiconducting gas sensors, transparent electrode material in DSSCs and LEDs, antiferromagnetic material in ReRAM, etc. [1–4].

Among various methods of NiO layers formation, metal-organic chemical vapor deposition (MOCVD) is of particular interest because it provides formation of high quality coatings on the substrates with complicated shape. However, the amount of Ni-containing compounds suitable for MOCVD is limited to a few metal-organic compounds such as nickel carbonyl [5], Ni β-diketonates and their derivatives [6–12], and bis-π-cyclopentadienyl compounds [13–15]. Nickel carbonyl is extremely toxic. It has been shown that NiO layers can be deposited with relatively high growth rate (up to 300 nm/h) from β-diketonates in the temperature range 500–800 K under reduced pressure. However, the authors noted that Ni/O ratio in the films can be varied over a wide range and significant amount of carbon was found in the deposits. In the case of bis-π-cyclopentadienyl compounds and oxidants used as precursors, one can deposit high-quality layers at 550 K with growth rates of about 100 nm/h. However, the authors studied the kinetic regularities of the layer formation only, disregarding the transformations of precursors in the gas phase.

The successful use of bis-(ethylcyclopentadienyl)nickel $(EtCp)_2Ni$ for MOCVD of NiO layers using O_2 and O_3 was demonstrated for the first time [16–19]. The results from an experimental study [17] showed that thermally activated MOCVD of NiO layers in the reaction systems $(EtCp)_2Ni–O_2–Ar$ and $(EtCp)_2Ni–O_2–O_3–Ar$ was kinetically controlled in the temperature range of 600–740 K. The corresponding value of apparent activation energy of the processes in this temperature range was 80 ± 5 kJ·mol^{-1} for both reaction systems. In the temperature region 740–840 K, the value of apparent activation energy was 18 ± 7 kJ·mol^{-1}. However, introduction of ozone led to nearly 2-fold decrease of NiO layers deposition rate. Various circumstantial results indicated that the reduction of NiO layers growth rate in the presence of ozone could be caused by the simultaneous formation of gas-phase Ni-containing compounds that were not involved in the layers deposition process.

The main purpose of this work was an experimental study of gas-phase chemical transformations in the reaction systems $(EtCp)_2Ni–O_2–Ar$ and $(EtCp)_2Ni–O_3–O_2–Ar$ by means of time-of-flight mass-spectrometry, in order to gain a more clear understanding of the reaction mechanism of thermally activated MOCVD of NiO layers.

Correspondence to: Anastasia S. Kondrateva; *e-mail:* a_kondrateva@spbstu.ru

Experimental

Gas-phase reactions were carried out in the quartz tubular "hot wall" reactor under the following conditions: deposition zone temperature was 330–830 K, $(EtCp)_2Ni$ (97%, DalChem) molar flow rate was 1.8–4.7 μmol·min^{-1}, oxygen and ozone partial pressures were 30–330 Pa and 0–770 Pa, correspondingly, Ar flow rate was 25 sccm, total gas flow rate was 200 sccm, and total pressure was 840 Pa. Argon (Ar) was used as a carrier and diluent gas. The reactor inner diameter was 56 mm. Time of reactions was determined mainly by the residence time of the gas stream in hot zone of the reactor used. The estimated value of the residence time under conditions studied was about 0.1 s. Gas samples were fed to the mass-analyzer chamber through a heated sampling system to prevent deposition on the internal surfaces of the equipment. The experimental setup was described in detail [19]. Ozone was generated from oxygen (electronic grade) by special DBD generator. The ozone partial pressure was determined by using FTIR spectrometry [17]. Mass-spectrometric study of the reaction gas phase was carried out by using the reflectron-type time-of-flight (TOF) mass-spectrometer MSH-2282. Ionization energy was 100 eV. All mass-spectra were normalized to the amplitude of mass-peak at *m/z* 20 Da corresponding to the ion of argon (Ar^{++}).

X-ray photoelectron spectroscopy (SPECS HAS 3500) was used for chemical analysis. The presence of crystalline phases was investigated by means of X-ray diffraction [Super Nova Dual Wavelength (Agilent Technology), CuKα (λ = 1.5405 Å)].

Results and Discussion

Mass-Spectra of the Reaction Gas Phase

Despite of advantages of the use of $(EtCp)_2Ni$ as a precursor for MOCVD of NiO layers, reports on its studies are still comparatively rare. According to [18] a typical mass-spectrum of $(EtCp)_2Ni$ vapor (298 K, 10^5 Pa) can be represented in the form of four groups of peaks. The first group of mass peaks with *m/z* values 1–60 Da was determined not only by the fragmentation of the $(EtCp)_2Ni$ into light hydrocarbon ions, hydrogen, and atomic carbon, but also by the signal from residual gas. The second group of mass peaks (60–120 Da) corresponded to a number of cyclopentadienyl $[Cp]^+$ ions without nickel atom, with various substituents. The third group of mass peaks (120–250 Da) corresponded to various subsidiary ions of the molecular ion $[(EtCp)_2Ni]^+$. The fourth group of mass peaks (250–1000 Da) corresponded to various cluster ions of the $(EtCp)_2Ni$. The cluster ions consisted of Cp_2Ni, $Me(Cp)_2Ni$, $Et(Cp)_2Ni$, $MeEt(Cp)_2Ni$, $(MeCp)_2Ni$, and $(EtCp)_2Ni$ in various combinations. The intensities of cluster ions were very low compared with ion of parent molecule $(EtCp)_2Ni$; therefore one can suggest that their role in deposition process is unessential and transformation of those clusters will be not considered.

The transformations of $(EtCp)_2Ni$ began at approximately 375 K for all reaction systems (Figure 1). The $(EtCp)_2Ni$ conversion rate calculated by the change in the intensity of the parent molecular ion increased sharply with temperature in the reaction zone. The noticeable interaction of the initial $(EtCp)_2Ni$ and O_2 started at 430 K; interaction of the $(EtCp)_2Ni$ and O_3 started at 330 K. It is worth noting that pure Ni deposition rate [18, 19] was significantly lower than NiO deposition rate in the reaction systems $(EtCp)_2Ni–O_2–Ar$ and $(EtCp)_2Ni–O_3–O_2–Ar$, which corresponded to the lower $(EtCp)_2Ni$ conversion rate. However, the ozone introduction led to an increase of the conversion rate in comparison with the reaction system $(EtCp)_2Ni–O_2–Ar$ despite the nearly 2-fold decrease of NiO deposition rate. Apparently, this fact indicates the substantial role of transformations taking place in the reaction gas phase.

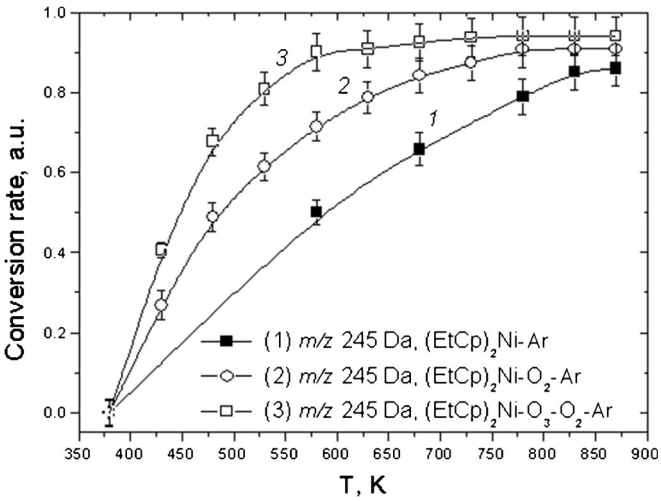

Figure 1. Temperature dependence of the conversion rate of $(EtCp)_2Ni$ in the reaction systems, (1) $(EtCp)_2Ni–Ar$, (2) $(EtCp)_2Ni–O_2–Ar$, and (3) $(EtCp)_2Ni–O_3–O_2–Ar$

Gas-Phase Transformations in the Reaction System $(EtCp)_2Ni–O_2–Ar$

The comparison of the reaction systems $(EtCp)_2Ni–Ar$ and $(EtCp)_2Ni–O_2–Ar$ (Table 1, col. 2 and 3) mass spectra obtained under similar conditions showed that introduction of O_2 caused appearance of mass peaks with *m/z* 29, 46, 52, 80, 110, 217, and 277 Da, probably corresponding to new substances formed in the presence of O_2 in the gas phase at 380–700 K.

The appearance of these mass peaks may be adequately explained taking into account the existence of two main reaction pathways for interaction between the substituted Cp compounds with O_2. The former is acid formation [20, 21], the latter is oxide formation [22].

The formation of the Ni-containing acid from $(EtCp)_2Ni$ may be described as (Equation 1):

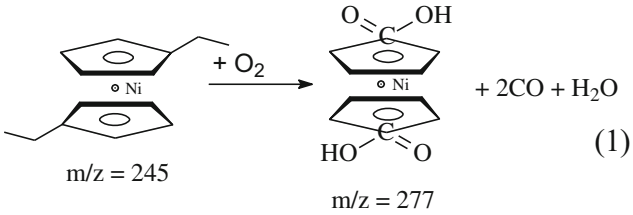

(1)

Table 1. Mass peaks and Their Identification for Reaction Systems $(EtCp)_2Ni$–Ar, $(EtCp)_2Ni$–O_2–Ar, and $(EtCp)_2Ni$–O_3–O_2–Ar

	$(EtCp)_2Ni$–Ar	$(EtCp)_2Ni$–O_2–Ar	$(EtCp)_2Ni$–O_3–O_2–Ar
m/z, Da	Ion		
2	H_2^+	H_2^+	H_2^+
14	CH_2^+	CH_2^+	CH_2^+
18	H_2O^+	H_2O^+	H_2O^+
28	N_2^+, CO^+	N_2^+, CO^+	N_2^+, CO^+
29		HCO^+	HCO^+
32	O_2^+	O_2^+	O_2^+
36	C_3^+	C_3^+	C_3^+
39			c-$C_3H_4^+$
40	Ar^+, $C_3H_4^+$	Ar^+, $C_3H_4^+$	Ar^+, $C_3H_4^+$
44	CO_2^+	CO_2^+	CO_2^+
46		$C_2H_4OH^+$	$C_2H_4OH^+$
52		c-$C_4H_4^+$	c-$C_4H_4^+$
56	$C_4H_8^+$	$C_4H_8^+$	$C_4H_8^+$
58			$C_2H_2O_2^{\bullet}$
65	$Cp^{\bullet}$	$Cp^{\bullet}$	$Cp^{\bullet}$
68			$C_4H_4O^{\bullet}$
79	$MeCp^{\bullet}$	$MeCp^{\bullet}$	$MeCp^{\bullet}$
80		$CpO^{\bullet}$	$CpO^{\bullet}$
93	$EtCp^{\bullet}$	$EtCp^{\bullet}$	$EtCp^{\bullet}$
100			$C_5H_8O_2^{\bullet}$
110		$CpCOOH^{\bullet}$	$CpCOOH^{\bullet}$
124	$[CpNi]^{\bullet}$	$[CpNi]^{\bullet}$	$[CpNi]^{\bullet}$
126			$C_7H_{10}O_2^{\bullet}$
152	$[EtCpNi]^{\bullet}$	$[EtCpNi]^{\bullet}$	$[EtCpNi]^{\bullet}$
189	$(Cp)_2Ni^{\bullet}$	$(Cp)_2Ni^{\bullet}$	$(Cp)_2Ni^{\bullet}$
193			$(C_4H_3O)_2Ni^{\bullet}$
217	$Et(Cp)_2Ni^{\bullet}$	$(CpO)_2Ni^{\bullet}$	$(CpO)_2Ni^{\bullet}$
231	$MeEt(Cp)_2Ni^{\bullet}$	$MeEt(Cp)_2Ni^{\bullet}$	$MeEt(Cp)_2Ni^{\bullet}$
245	$(EtCp)_2Ni^{\bullet}$	$(EtCp)_2Ni^{\bullet}$	$(EtCp)_2Ni^{\bullet}$
277		$(CpCOOH)_2Ni^{\bullet}$	$(CpCOOH)_2Ni^{\bullet}$
289			$EtCpNiEtCpO_3^{\bullet}$
337			$EtCpO_3NiEtCpO_3^{\bullet}$

The occurrence of this reaction was confirmed by the decrease in the initial $(EtCp)_2Ni$ mass peak intensity with the O_2 introduction and by the appearance of the mass peaks corresponding to the reaction product $(CpCOOH)_2Ni$ or its fragments since $(CpCOOH)_2Ni$ dissociates with formation of cyclopentadiene carboxylic acid CpCOOH and NiO (Equation 2):

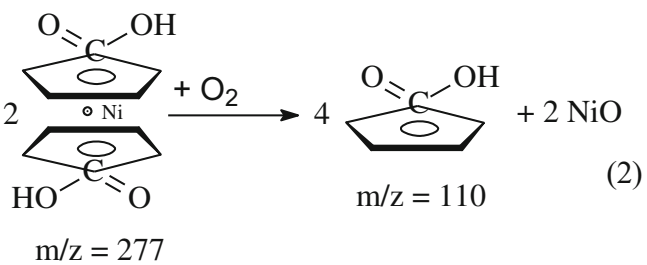

(2)

Temperature dependence of the mass peak *m/z* 110 Da intensity corresponding to the gas-phase $(CpCOOH)_2Ni$ dissociation product (2) is shown (Figure 2). The increase in 110 Da mass peak intensity was attributable to the enhancement of the "$(EtCp)_2Ni$–O_2" interaction with temperature increasing up to 670 K. The decrease of mass peak intensity with the further temperature rise was caused by the $(EtCp)_2Ni$ concentration decline due to its thermal decomposition in the reactor zone situated prior to the reaction zone [23].

CpCOOH [24] thermally dissociates with formation of CO, CO_2, and cyclobutadiene c-C_4H_4 when temperature exceeds 700 K (Equation 3):

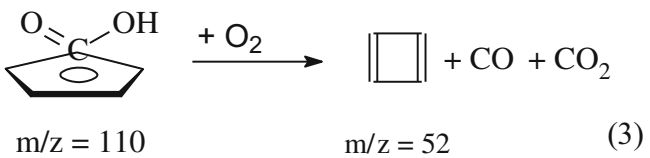

(3)

CpCOOH dissociation resulted in the increasing intensity of the mass peaks corresponding to the ionized reaction products with temperature (Figure 3).

At these temperatures, cyclobutadiene can interact with O_2 undergoing various transformations [25–27]. Under given conditions, the most probable products of "c-C_4H_4–O_2" interaction are formyl HCO and ethyl alcohol C_2H_5OH. This suggestion was supported by the presence of corresponding mass peaks *m/z* 29 and 46 Da in mass spectra (Figure 4).

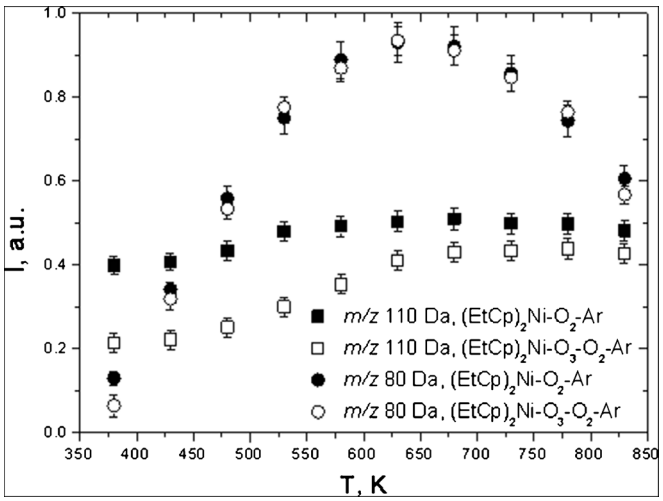

Figure 2. Temperature dependence of the *m/z* 80 and 110 Da intensities

Interaction between the substituted Cp compounds with O_2 with formation of cyclopentadienones [20, 28, 29] in the case of $(EtCp)_2Ni$ may be described as (Equation 4):

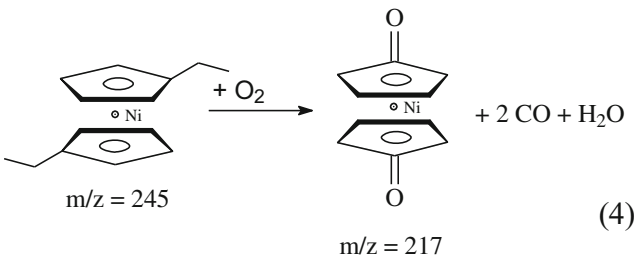

(4)

Bis-(cyclopentadienonyl) nickel $(CpO)_2Ni$ may also participate in NiO layers formation by dissociation (Equation 5) into the cyclopentadiene oxide CpO and NiO:

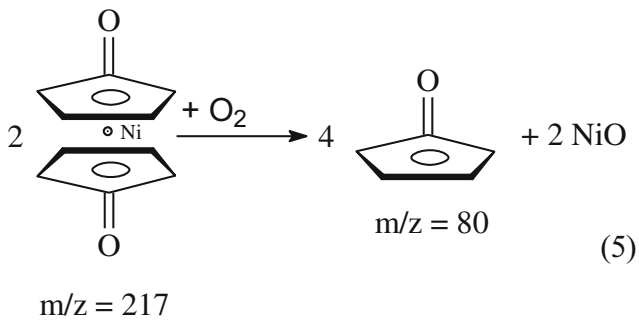

(5)

The occurrence of $(CpO)_2Ni$ dissociation was confirmed by the increase in mass peak 80 Da intensity with temperature rising up to 700 K in the deposition zone (Figure 2). CpO is thermally decomposed above 700 K.

The analysis of the mass spectra of gas phase formed above 630 K indicated the appearance of mass peaks *m/z* 42, 56, and 84 Da. This fact suggests that reaction scheme could be changed because of a substantial fragmentation of the gas-phase

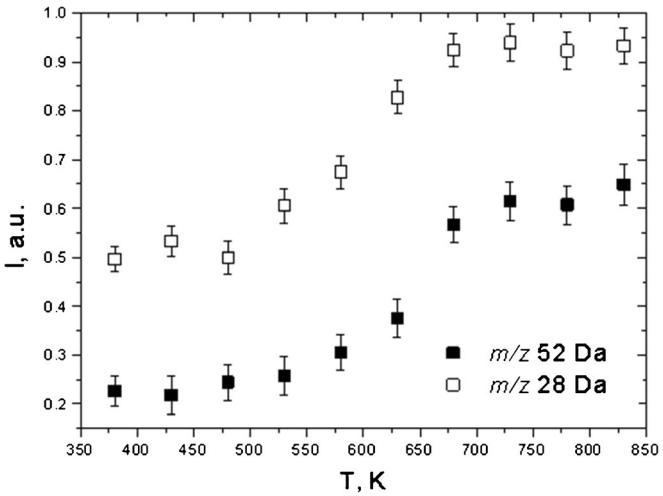

Figure 3. Temperature dependence of the *m/z* 28 and 52 Da intensities

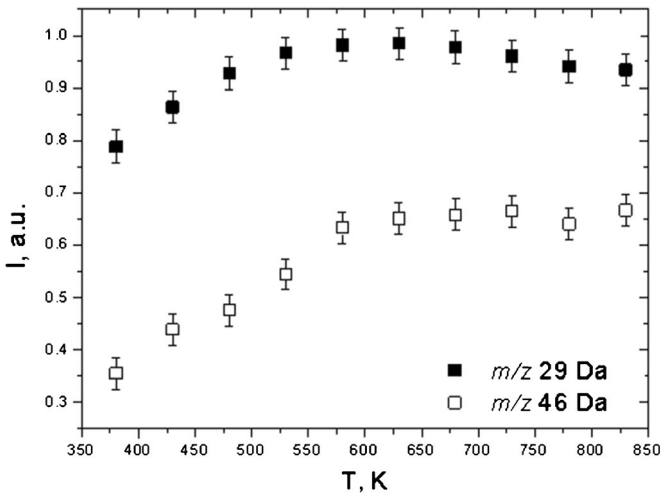

Figure 4. Temperature dependence of the *m/z* 29 and 46 Da intensities

components resulting in the increase in the amount of light hydrocarbons formed. At high temperatures [30–32] the Cp radicals more likely undergo ring opening reactions via breaking C(1)-C(5), C(2)-C(3), or C(3)-C(4) bonds [27, 33]. Thus, the additional mass-peaks *m/z* 42, 56, and 84 Da are likely signals belonging to ethenone C_2H_2O, acrolein C_3H_4O, and ethyl vinyl ketone C_5H_8O, respectively, formed by breaking of Cp double bonds in an oxidizing atmosphere (Equation 6):

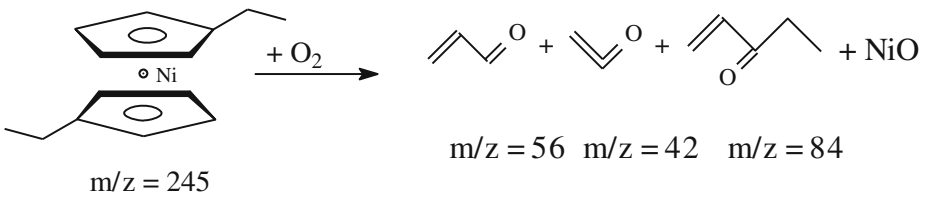

(6)

This process is enhanced by the temperature rise in the reaction zone, which results in the increase of corresponding mass peak intensity (Figure 5).

Pearson's correlation coefficients k [34, 35] for mass peak pairs corresponding to the reagents and products of some reactions described have been calculated at different temperatures to clarify the processes of temperature ranges. The coefficient *k* calculated for *m/z* 245 and *m/z* 110 Da was $k < -0{,}75$ at the temperatures below 550 K. Thus, increase in the intensity of mass peak at 245 Da is followed by decrease in intensity of mass peak at 110 Da, i.e., they are highly negatively correlated according to the Chaddock's scale. The same patterns were revealed for mass-peak pairs 245–80 Da ($k < -0{,}5$) and 245–29 Da ($k < -0{,}86$), whereas mass peak intensities for pairs 110–80 Da and 110–29 Da were highly positively correlated with temperature rise up to 600 K. Pearson's coefficients for mass peak pairs 245–42 Da and 245–29 Da ($k < -0{,}75$) are negative and high above 630 K, i.e., increase in the intensity of mass peak at 245 Da is followed by decrease in the intensity of mass peaks at 42 and 29 Da. Pearson's coefficient for 42–29 Da ($k > 0{,}5$) is high. Therefore, it is possible to conclude that $(EtCp)_2Ni$ undergoes transformations in accordance with the afore-cited.

The research performed showed that the perceptible interaction of the initial $(EtCp)_2Ni$ with O_2 started at 430 K. The formation of gas-phase bis-(cyclopentadienylcarboxy) nickel and bis-(cyclopentadienonyl) nickel was found in the low temperature region in addition to NiO layers deposition. The ring opening processes leading to the formation of a large amount of light hydrocarbons (formyl, ethanol, ethenone, acrolein, ethyl vinyl ketone) and carbon oxides were found to prevail above 630 K.

Gas-Phase Transformations in the Reaction System $(EtCp)_2Ni–O_3–O_2–Ar$

The comparison of mass spectra of the reaction systems $(EtCp)_2Ni–O_2–Ar$ and $(EtCp)_2Ni–O_3–O_2–Ar$ (Table 1, col. 3 and 4) obtained under similar conditions showed that O_3 introduction initiated the appearance of mass peaks *m/z* 39, 58, 68, 100, 126, 193, 289, and 337 Da, whereas the intensity of the mass peak *m/z* 110 Da corresponding to CpCOOH decreased distinctly. Temperature dependencies of the mass peaks *m/z* 80 and 110 Da intensities with and without O_3 are shown (Figure 2). Comparison of corresponding mass peaks intensities indicated that O_3 introduction reduced the CpCOOH formation probability and had no effect on the CpO formation.

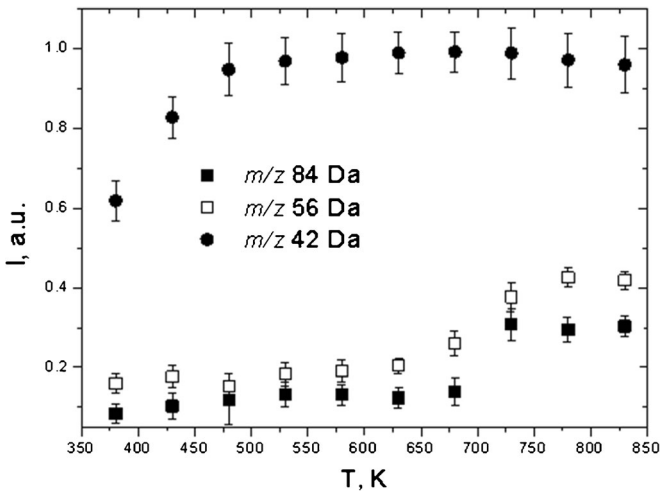

Figure 5. Temperature dependence of the *m/z* 42, 56, and 84 Da intensities

Interaction of aromatics with O_3 in the gas phase leads to the formation of ozonides, which subsequently undergo decomposition or stabilization [36–40]. Moreover, it is shown that no additional activation is needed for interaction of O_3 and aromatics double bonds [41], [42]. Taking these facts into account, it may be suggested that O_3 molecule attacks the Cp double bond in $(EtCp)_2Ni$ with formation of ozonide of the latter (*m/z* 289 and 337 Da) via (Equations 7, 8).

In the case of dissociation, the ozonide (*m/z* 337 Da) is decomposed into ethyl pentenedial (*m/z* 126 Da) (Equation 9). Similarly, O_3 can attack the double bond in ethyl pentenedial to form an ozonide (Equation 10) subsequently decomposing into ethyl propanedial (*m/z* 100 Da) and ethanedial (*m/z* 58 Da) (Equation 11). The suggested scheme of transformations was confirmed by the presence in the mass spectra of afore-cited mass peaks, apparently indicating the ethanedial, ethyl propanedial, and ethyl pentenedial formation.

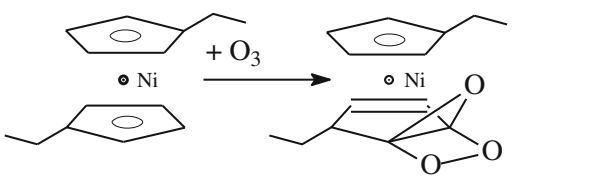

m/z = 245 m/z = 289 (7)

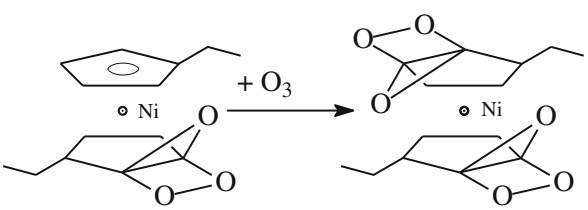

m/z = 289 m/z = 337 (8)

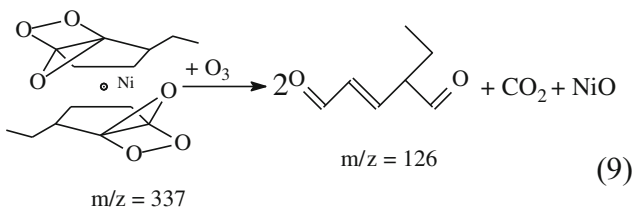

m/z = 337 m/z = 126 (9)

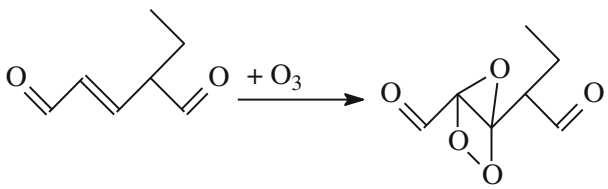

m/z = 126 m = 172 (10)

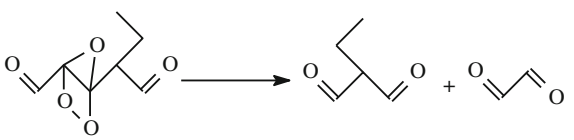

m = 172 m/z = 100 m/z = 58 (11)

The decrease of mass peaks *m/z* 58, 100, and 126 Da intensities (Figure 6) with temperature in the reaction zone indicates the reduction of the dialdehydes formation rate, which might be caused by decrease in O_3 partial pressure attributable to its thermal decomposition [42] above 630 K.

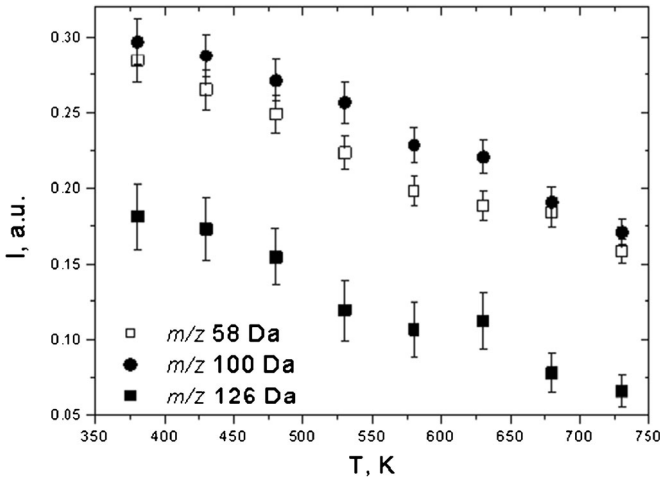

Figure 6. Temperature dependence of the *m/z* 58, 100, and 126 Da intensities

In the case of stabilization, the ozonide (*m/z* 337 Da) transforms into $(C_4H_3O)_2Ni$ (*m/z* 193 Da) (Equation 12):

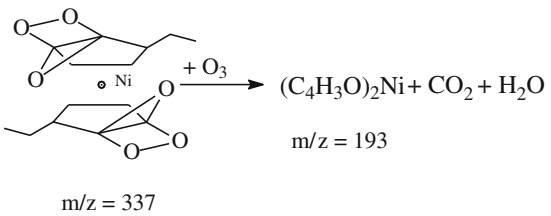

(12)

The occurrence of ozonide stabilization was confirmed by the appearance of the mass peaks corresponding to $(C_4H_3O)_2Ni$ (*m/z* 193 Da) or its fragments (*m/z* 39 and 68 Da) (Figure 7). Electron impact ionization of $(C_4H_3O)_2Ni$ resulted in the appearance of the same set of fragment ions as obtained by ionization of furan [43, 44]. $(C_4H_3O)_2Ni$ is unlikely to be involved in NiO layer deposition process. Thus, experimentally obtained reduction of NiO layers growth rate in the presence of O_3 could be attributed to the precursor concentration decrease as a result of $(C_4H_3O)_2Ni$ formation.

The Pearson's correlation coefficient calculated for 245–193 and 245–68 Da was $k > 0.63$ above 380 K. Thus, decrease in the intensity of mass-peak at 245 Da was followed by decrease in the intensity of *m/z* 68 and 193 Da. The Pearson's coefficient for 193–68 Da was $k > 0.89$ at all temperatures considered. Fragments with *m/z* 193–68 Da are likely to be formed below 380 K (up to the deposition zone at the mixing point), which is confirmed by the O_3 thermal resistance data (Figure 8).

On the basis of the results from a study of the reaction, gas phase formed in the reaction systems $(EtCp)_2Ni–O_2–Ar$ and $(EtCp)_2Ni–O_3–O_2–Ar$ model reaction scheme illustrating some transformation of the precursor $(EtCp)_2Ni$ has been developed (Figure 8). The perceptible interaction of the initial $(EtCp)_2Ni$ and ozone was established to start at 330 K. Dialdehydes (ethanedial, ethyl propanedial, and ethyl pentenedial) and $(C_4H_3O)_2Ni$ are formed at 330–380 K. Mainly the same gas-phase species as in the reaction system $(EtCp)_2Ni–O_2–Ar$, i.e., bis-(cyclopentadienylcarboxy) nickel and bis-(cyclopentadienonyl) nickel, were formed above 380 K. A large amount of light hydrocarbons (formyl, ethanol, ethenone,

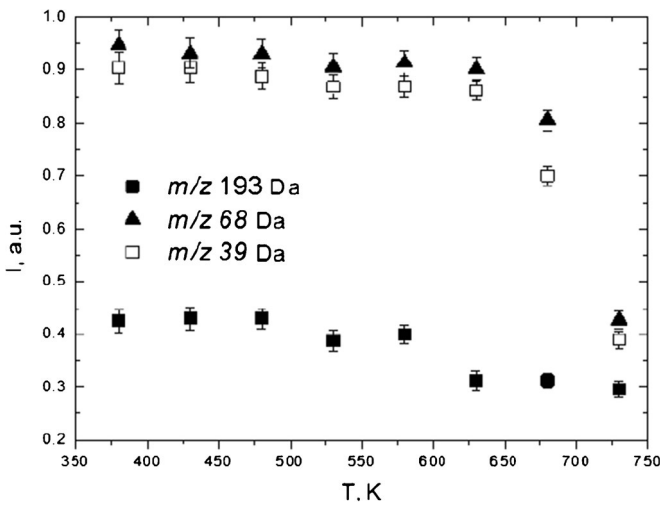

Figure 7. Temperature dependence of the *m/z* 39, 68, and 193 Da intensities

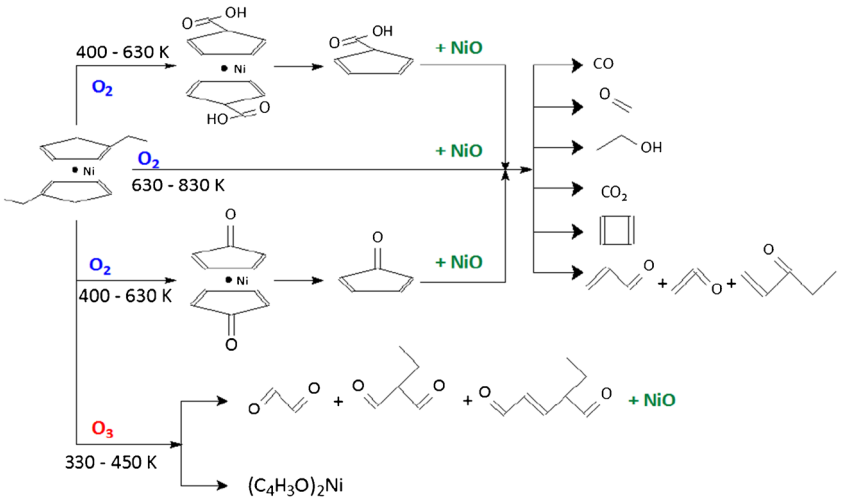

Figure 8. The model reaction scheme illustrating $(EtCp)_2Ni$ transformations

acrolein, ethyl vinyl ketone) and carbon oxides was formed above 630 K.

Chemical Composition and Morphology of Deposited Layers

The XPS patterns of the deposited NiO layers indicate formation of NiO with almost stoichiometric composition (O/Ni in the range 0.98–1.03) for both reaction systems studied. All of the deposited NiO layers did not contain any carbon contamination in significant amounts (less than 1%).

The results of XRD study show that the films are characterized by preferential (100) orientation of crystallites. The calculated value of lattice parameter (4.17 ± 0.015 Å) did not depend on the deposition conditions and was close to the value of bulk NiO bunsenite (4.18 Å) with cubic face-centered lattice. The ICDD card number is 71–4751.

Conclusions

On the basis of the results from mass-spectrometric study of the reaction gas phase formed during MOCVD of NiO layers in the reaction systems $(EtCp)_2Ni–O_2–Ar$ and $(EtCp)_2Ni–O_3–O_2–Ar$ reaction scheme of the deposition process was developed.

It is most probable that formation of NiO layers in the reaction system $(EtCp)_2Ni–O_2–Ar$ in the temperature range 380–600 K occurs via formation of intermediate products of gas-phase oxidation of the precursor: bis-(cyclopentadienylcarboxy) nickel and bis-(cyclopentadienonyl) nickel. NiO layers can be formed either as a result of the following bis-(cyclopentadienylcarboxy) nickel dissociation into cyclopentadiene carboxylic acid and NiO or through bis-(cyclopentadienonyl) nickel dissociation into cyclopentadiene oxide and NiO. $(EtCp)_2Ni$ more likely undergoes ring opening reactions via breaking Cp double bonds above 630 K leading to the formation of formyl, ethyl alcohol, ethenone, acrolein, and ethyl vinyl ketone in addition to NiO layers.

It was found that in the reaction system $(EtCp)_2Ni–O_3–O_2–Ar$ at 330–600 K apart from the above-mentioned mechanisms of NiO formation, nickel oxide can be formed via intermediate formation of $(EtCp)_2Ni$ ozonide, which dissociates into dialdehydes (ethanedial, ethyl propanedial, and ethyl pentenedial) and NiO. Besides, ozone introduction leads to the gas-phase formation of $(C_4H_3O)_2Ni$, which is unlikely to be involved in formation of NiO; however, it causes the depletion by the precursor in the gas phase, and this is confirmed by the experimentally found 2-fold decrease of NiO deposition rate in this reaction system.

References

1. Rödl, C., Schleife, A.: Photoemission spectra and effective masses of n- and p-type oxide semiconductors from first principles: ZnO, CdO, SnO2, MnO, and NiO. Phys. Status Solidi A **81**(1), 74–81 (2014)
2. Houari, S., Nguyen, D., Jouan, P., Khelil, A., Mokrani, A., Cattin, L., Predeep, P., Berne, J.C.: Because, Introduction: XPS study of the band alignment at ITO/oxide (n-type MoO3 or p-type NiO) interface. Phys. Status Solidi A **7**, 1–7 (2012)
3. Chen, Yongyue., Sun, Yajie., Dai, Xusheng., Zhang, Bingpo., Ye, Zhenyu., Wang, Miao., Wu, Huizhen: Tunable electrical properties of NiO thin fi lms and p-type thin- film transistors. Thin Solid Films **592**, Elsevier B.V., 195–199 (2015)
4. Schulz, Philip., Whittaker-brooks, Luisa L., Macleod, Bradley A., Olson, Dana C., Loo, Yueh-lin., Kahn, Antoine: Electronic Level Alignment in Inverted Organometal Perovskite Solar Cells. (2015)
5. Paserin, B.V., Marcuson, S., Shu, J., Wilkinson, D.S.: CVD technique for inco Nickel foam production. Adv. Eng. Mater. **6**, 454–459 (2004)
6. Andrew, A., Johnson, L., Cosham, S.D., Stephen, P., Manning, T., Hill, M.S., Molloy, K.C., Cosham, S.D., Richards, S.P.U.A.: Precursors for p - type Nickel Oxide : Atmospheric Pressure MOCVD of Nickel Oxide thin films with high work functions. Eur. J. Inorg. Chem. **13**, 1868–1876 (2017)
7. Battiato, S., Giangregorio, M.M., Catalano, M.R., Nigro, L.: Morphology-controlled synthesis of NiO fi lms : the role of the precursor and the effect of the substrate nature on the films structural / optical properties. RSC Adv. **6**, 30813–30823 (2016)
8. Moravec, P.: NiOx nanoparticle synthesis by chemical vapor deposition from nickel acetylacetonate. Mater. Sci. Appl. **2**(4), 258–264 (2011)

9. Meersschauta, J., Toellerb, M., Schaekersa, M., Wanga, X.P., Brijsa, B., Woutersa, D.J., Jurczaka, M., Altimimea, L., Van Elshochta, S., Vancoille, E.: Metal-organic chemical vapor deposition of Ti-doped NiO layers for application in resistive switching memories. J. Meersschaut. ECS Trans. **33**(3), 313–322 (2010)
10. Basato, M., Faggin, E., Tubaro, C., Cesare, A.: Volatile square planar b - imino carbonyl enolato complexes of Pd (II) and Ni (II) as potential MOCVD precursors. Polyhedron 28, Elsevier Ltd. **7**, 1229–1234 (2009)
11. Min, K.C., Kim, M., You, Y.H., Lee, S.S., Lee, Y.K., Chung, T.M., Kim, C.G., Hwang, J.H., An, K.S., u. a.: NiO thin films by MOCVD of $Ni(dmamb)_2$ and their resistance switching phenomena. Surf. Coat. Technol. **201**(22–23), 9252–9255 (2007)
12. Malandrino, G., Perdicaro, L.M., Condorelli, G., Fragala, I.L., Rossi, P., Dapporto, P.: Synthesis, characterization and application of Ni (tta) 2· tmeda to MOCVD of nickel oxide thin films. Dalton Transactions **8**, 1101–1106 (2006)
13. Roffi, T.M., Nozaki, S., Uchida K.: Growth mechanism of single-crystalline NiO thin films grown by metal organic chemical vapor deposition. J. Crystal Growth **451**, 57–64 (2016)
14. Antony Premkumar, P., Toeller, M., Adelmann, C., Meersschaut, J., Franquet, A., Richard, O., Tielens, H., Brijs, B., Moussa, A., u. a.: NiO thin films synthesized by atomic layer deposition using $Ni(dmamb)_2$ and ozone as precursors. Chem. Vap. Depos. **18** (1–3), 61–69 (2012)
15. Kimbell, M.: Chemical vapor deposition of nickel ferrite using Ni (C5H5)2 and fe(C5H4C4H9)(C5H5). J. Undergrad. Res. **1**, 4–8 (2010)
16. Kondrateva, A.S., Alexandrov, S.E.: Vac. Tech. Vac. Technol. **23**(1), 106–107 (2014)
17. Kondrateva, A., Mishin, M., Shakhmin, A., Baryshnikova, M., Alexandrov, S.E.: Kinetic study of MOCVD of NiO films from bis-(ethylcyclopentadienyl) nickel. Phys. Status Solidi C. **12**, 912–917 (2015)
18. Alexandrov, S.E., Protopopova, V.S.: Chemical vapor deposition of Ni–C films from bis-(ethylcyclopentadienyl). Nickel **11**, 8259–8263 (2011)
19. Protopopova, V.S., Alexandrov, S.E.: Mass-spectrometric and kinetic study of Ni films MOCVD from bis-(ethylcyclopentadienyl) nickel. Surf. Coat. Technol. **230**, 316–321 (2013)
20. Sebbar, N., Bozzelli, J.W., Bockhorn, H.: Thermochemistry and kinetics for 2-Butanone-1-yl radical (CH2·C(O)CH2CH3) (CH2·C(O)CH2CH3) reactions with O2. J. Phys. Chem. A **118**(1), 21–37 (2014)
21. Brezinsky, K.: The high-temperature oxidation of aromatic hydrocarbons. Prog. Energy Combust. Sci. **12**(1), 1–24 (1986)
22. Robinson, R.K.., Lindstedt, R.P.: On the chemical kinetics of cyclopentadiene oxidation. Combust. Flame. **158** (4), 666–686 (2011)
23. Hansen, N., Klippenstein, Stephen. J., Miller, J.A., Wang, J., Cool, T.A., Law, M.E., Westmoreland, P.R., Kasper, T., Kohse-Höinghaus, K.: Identification of C5Hx isomers in fuel-rich flames by photoionization mass spectrometry and electronic structure calculations. J. Phys. Chem. A **110** (13), 4376–4388 (2006)
24. Norinaga, K., Deutschmann, O.: Detailed kinetic modeling of gas-phase reactions in the chemical vapor deposition of carbon from light hydrocarbons. Ind. Eng. Chem. Res. **46**(11), 3547–3557 (2007)
25. Chen, C.-J., Bozzelli, J.W.: Analysis of tertiary butyl radical + O_2, Isobutene + HO_2, Isobutene + OH, and Isobutene - OH Adducts + O_2: a detailed tertiary butyl oxidation mechanism. J. Phys. Chem. A **103**, 9731–9769 (1999)
26. Laskin, A., Wang, H.A.I., Law, C.K.: Detailed kinetic modeling of 1, 3-butadiene oxidation at high temperatures. Int. J. Chem. Kinet. **32**, 589–614 (2000)
27. Kidwell, N.M., Vaquero-vara, V., Ormond, T.K., Buckingham, G.T., Zhang, D., Mehta-hurt, D.N., Mccaslin, L., Nimlos, M.R., Daily, J.W.U.A.: Chirped-pulse fourier transform microwave spectroscopy coupled with a flash pyrolysis microreactor: structural determination of the reactive intermediate cyclopentadienone. J. Phys. Chem. Lett. **5**, 2201–2207 (2014)
28. Wang, H., Brezinsky, K.: Computational study on the thermochemistry of cyclopentadiene derivatives and kinetics of cyclopentadienone thermal decomposition. J. Phys. Chem. A **102**(9), 1530–1541 (1998)
29. Claeys, M., Wang, W., Ion, A.C., Kourtchev, I., Gelencsér, A., Maenhaut, W.: Formation of secondary organic aerosols from isoprene and its gas-phase oxidation products through reaction with hydrogen peroxide. Atmos. Environ. **38**(25), 4093–4098 (2004)
30. Vourliotakis, G., Skevis, G., Founti, M.A., Vourliotakis, G., Skevis, G., Founti, M.A.: A detailed kinetic modelling study of benzene oxidation and combustion in premixed flames and ideal reactors. Energy Fuels **25**(5), 1950–1963 (2011)
31. Buda, F., Heyberger, B., Fournet, R., Glaude, P.A., Warth, V., Battin-Leclerc, F.: Modeling of the gas-phase oxidation of cyclohexane. Energy Fuels **20**(4), 1450–1459 (2006)
32. Metcalfe, W.K., Dooley, S., Dryer, F.L.: Comprehensive detailed chemical kinetic modeling study of toluene oxidation. Energy Fuel **25**(11), 4915–4936 (2011)
33. Butler, R.G., Glassman, I.: Cyclopentadiene combustion in a plug flow reactor near 1150 K. P. Combustion Instit. 32 I, Combust. Instit. **1**, 395–402 (2009)
34. Kyle Wickings, A., Grandy, S., Reed, S.C., Cory, C.: The origin of litter chemical complexity during decomposition. Ecol. Lett. **15**, 1180–1188 (2012)
35. Castellanos, M., Campos, F., Rodr, M., Blanco, M., Arias, S.: Blood levels of glutamate oxaloacetate transaminase are more strongly associated with good outcome in acute ischaemic stroke than glutamate pyruvate transaminase levels. Clin. Sci. **17**, 11–17 (2011)
36. Horie, O., Moortgat, G.K., Planck, M.: Gas-phase ozonolysis of alkenes. Recent advances in mechanistic investigations. Acc. Chem. Res. **31**(7), 387–396 (1998)
37. Neal, H.E.O., Blumstein, C.: A new mechanism for gas phase phase ozone-olefin. Int. J. Chem. Kinet. **5**, 397–413 (1973)
38. Carer, L: Kinetics and mechanisms of the gas-phase reactions of ozone with organic compounds under atmospheric conditions. Chem. Rev. **84**, 437–470 (1984)
39. Zhou, J., Zhao, Q., Chen, W.-W., Wang, H., Lin, G.-Q., Xu, M.-H., Guo, Y.: Studies on gas-phase cyclometalations of ArNi(PPh3)n. + (n = 1 or 2) by electrospray ionization tandem mass spectrometry. J. Am. Soc. Mass Spectromet. **21**(7), 1265–1274 (2010)
40. Zhong, X., Bozzelli, J.W.: Thermochemical and kinetic analysis of the H, OH, HO2, O, and O-2 association reactions with cyclopentadienyl radical. J. Phys. Chem. A **102**(20), 3537–3555 (1998)
41. Martinez, R.I., Herron, J.T., Huie, R.E.: The mechanism of ozone-alkene reactions in the gas phase. a mass spectrometric study of the reactions of eight linear and branched-chain alkenes. J. Am. Chem. Soc. **103**, 3807–3820 (1981)
42. Alexandrov, S.E., Filatov, L.A., Protopopova, V.S., Baryshnikova, M.V.: Effect of ozone on deposition of titanium oxide films from tetraisopropoxide. ECS Trans. **25**(8), 381–387 (2009)
43. Nie, S.-P., Huang, J.-G., Zhang, Y.-N., Hu, J.-L., Wang, S., Shen, M.-Y., Li, C., Marcone, M.F., Xie, M.-Y.: Analysis of furan in heat-processed foods in China by automated headspace gas chromatography–mass spectrometry (HS-GC-MS). Food Control **30**(1), 62–68 (2013)
44. Opitz, J.: Electron impact ionization of dicyclopentadienyl- manganese and cyclopentadienyl- manganese-tricarbonyl compared with dimanganese- decacarbonyl : appearance energies, bond energies and enthalpies of formation. Eur. J. Mass Spectrom. **62**(7), 55–62 (2001)